Proceedings of the 25th International Conference on
Port and Ocean Engineering under Arctic Conditions
June 9-13, 2019, Delft, The Netherlands

Estimating icebergs hazards in the Barents Sea using a numerical iceberg drift and deterioration model

Edmond Hansen[1], Juliane Borge[1], Martin Arntsen[1], Andreas Olsson[2], and Mark Thomson[2]
[1] Multiconsult, Tromsø, Norway
[2] OMV Norge AS, Stavanger, Norway

ABSTRACT

The probability of iceberg occurrence is a major driver for the choice and design of concepts for exploitation of hydrocarbon resources in the northern parts of the Barents Sea. The sparse data on iceberg occurrence in the Barents Sea is therefore a complicating factor. Iceberg drift and deterioration models are able to deliver a wealth of relevant data, such as occurrence probabilities, size distributions, drift speed distributions, and so on. At the same time, the representativity of the results are difficult to assess. The effect of uncertainties in the forcing data and the model parameterizations may be quantified by ensemble modeling techniques, to the extent computational time allows such exercises to be carried out. However, when estimating iceberg occurrence probabilities, the results are sensitive to the numbers of icebergs being released to the Barents Sea from the production sites at Svalbard, Franz Josef Land and Novaja Zemlja. These numbers are unknown. In this paper we present a study where a numerical iceberg drift and deterioration model is used to produce a hindcast archive for iceberg trajectories in the Barents Sea. Based on the hindcast dataset, iceberg occurrence probabilities are calculated for the Wisting oil and gas field. The inherent uncertainties and sensitivities are quantified, and the applicability of the results in practical design is discussed in this context.

KEY WORDS: Iceberg; Occurrence; Probability; Modelling; Barents Sea

INTRODUCTION

Updated data on glacial ice occurrence in the Barents Sea are known to be sparse. Russian data covering the period 1881-1993 is the only known source of consistent iceberg observations (Abramov and Tunik, 1996). The most updated assessment report on the cryosphere (SWIPA, Sharp et al., 2011) does not contain information indicating that iceberg frequencies in the Abramov and Tunik (1996) atlas should be corrected in any direction due to recent climate change. It must nevertheless be acknowledged that the Abramov and Tunik (1996) data set – irrespective of its great value - contains uncertainties.

Until methodology based on remote sensing is reaching a level of sophistication allowing

operational applications to be developed, numerical modelling appears to be the most promising alternative source of information on iceberg statistics. Numerical modelling of iceberg drift and deterioration has reached advanced levels, following regular use of operational models in Canadian waters since the early 2000's (Kubat et al., 2005, 2007; Turnbull et al., 2015). Forcing such iceberg models with model hindcast data enables us to produce hindcast data of iceberg drift and deterioration in a region. Such hindcast drift and deterioration models have already been successfully set up for the Barents Sea (Broström et al., 2009, Keghouche et al., 2010).

On this background, numerical iceberg drift and deterioration modelling was carried out to determine iceberg occurrence probabilities in the northwestern Barents Sea. The results obtained from the numerical modeling work, should supplement the observational data in the Abramov and Tunik (1996) atlas. The modeling addresses iceberg occurrence probabilities at the location of the Wisting oil and gas field (73° 30' N 24° 14' E). The paper contains a brief description of the iceberg model as implemented for the purpose, its forcing data, and the resulting iceberg occurrence probability for the Wisting location.

MODEL AND FORCING DATA

Iceberg drift and deterioration model

A numerical iceberg drift and deterioration model for the Barents Sea was set up to serve the particular purposes of this project. The model includes all relevant physical forcing mechanisms, such as forces from air and water drag, wave forcing, force due to the interaction with sea ice, force due to the sea surface slope, and the Coriolis force. The model icebergs interact with the seabed. If they enter areas shallower than their draft, they remain grounded until they melt sufficiently to float off, or the air and water forcing changes direction so that the iceberg is forced back into deeper water. Finally, the modeled icebergs are deteriorating due to wave erosion and calving, as well as lateral and basal melting. The width to height-ratio of a particular iceberg may therefore change during its lifetime. If this ratio becomes smaller than a certain threshold, the iceberg will roll over. Following rollover, the iceberg width and height are swapped (following e.g. Stern et al., 2017). The iceberg geometry is taken into account where relevant. The model domain is shown in Figure 1.

The governing equations – with the associated parameterizations – are adapted from well-tested models like those of Kubat et al. (2005, 2007) and Keghouche et al. (2010). The modeling described by Keghouche et al. (2010) was made for the Barents Sea, and their choice of parameter values and the corresponding results are therefore particularly relevant. The iceberg rotation in the horizontal plane is not included in the model.

In this paper we focus on the principle of using a numerical model for the particular purpose of calculating occurrence probabilities. We present some first results and compare them to other studies. A detailed technical description of the iceberg model is therefore not included; due to paper length considerations we rather refer to Kubat et al. (2005, 2007) and Keghouche et al. (2010) for technical details on the model formulations.

Forcing data

Two hindcast datasets for wind, waves, currents and sea ice were used to force the model; ERA-Interim (Berrisford et al., 2011) and BaSIC4 (Røed et al., 2015). ERA-Interim is a global atmospheric reanalysis running over the period 1979-present, produced by the European Centre for Medium-Range Weather Forecasts (ECMWF). BaSIC4 is an ocean hindcast data set covering the Barents Sea region with 4 km resolution (Røed et al., 2015). The central metadata are summarized in Table 1, while the coverage is shown in Figure 1.

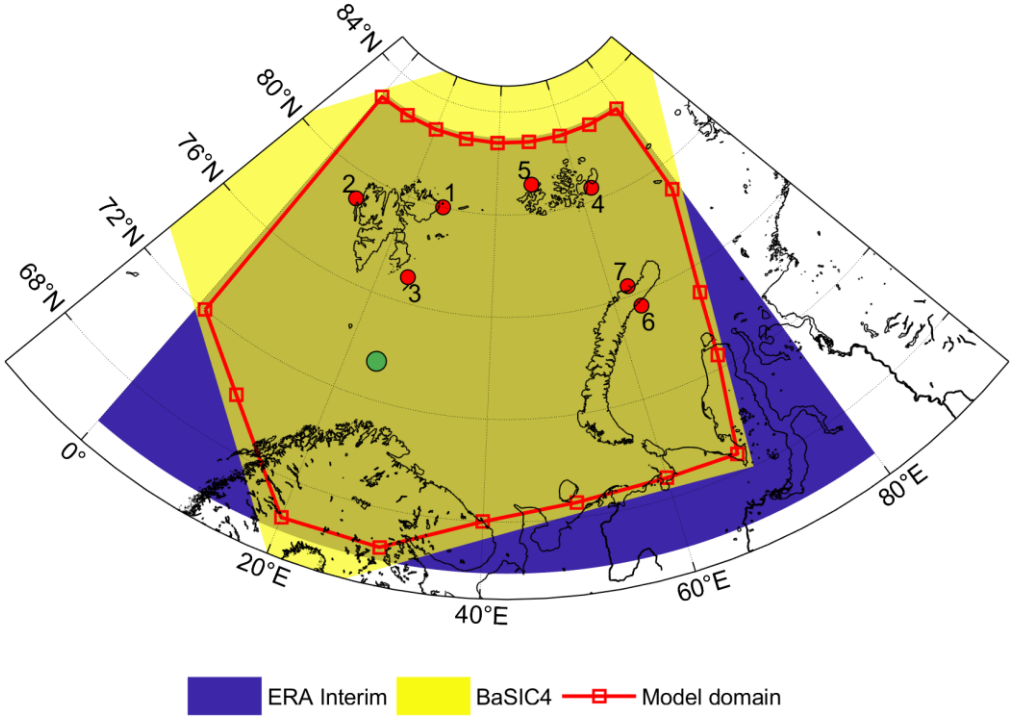

Figure 1 Input data and model domain: ERA Interim for Barents Sea area in blue, BaSIC4 domain in yellow, model domain as red polygon. Wisting is indicated with a green dot. The location of the iceberg release points are marked by red dots and numbered.

Table 1 Specifications of the hindcast forcing data, and parameters used to force the model.

	Time period available	**Resolution**	**Parameters used**
ERA Interim	01.01.1979-31.12.2017	Temporal: 6 hours, Spatial: approx. 80 km (T255 spectral), interpolated to 0.125° Resolution wave model: 1°, approx. 111 km	Wind speed and direction Air temperature Significant wave height, mean period
BaSIC4	01.01.1985-31.12.2012	Temporal: 1 hour Spatial: 4.2 km	Current speed and direction at 13 depth layers (0,10,20,30,40,50,60,70,80,90,100,125,150) Sea ice concentration, Sea ice drift speed, sea ice thickness Water temperature and salinity at surface

Iceberg characteristics

Icebergs are released at seven locations at Svalbard, Franz Josef Land, and Novaya Zemlya. Calving from Severna Zemlya, Ushakov Island and Victoria Island is neglected, as calving rates are small and it is unlikely that icebergs from these locations reach Wisting. We use the same calving rates as Keghouche et al. (2010), who summarized numbers provided in literature. There is considerable uncertainty in the percentage of the total volume of calved ice which

turns into icebergs in free drift in the Barents Sea. The calved ice may ground close to the glacier, melt and disintegrate close to their release area, or be released as growlers (L < 5 m). Keghouche et al. (2010) used a release rate of icebergs equivalent to 1 % of the total calved volume. Here we perform a comparison of the model results to the Abramov and Tunik (1996) atlas of icebergs, and adjust the release rate to obtain distribution patterns similar to those observed (described below).

Based on the average annual calving volume, a Poisson distribution is used to generate the volume that is released each year. Icebergs are released randomly throughout the year. Any seasonality in the results therefore stems from seasonality in the forcing. Glacier surges are not accounted for, due to the unavailability of data on number of released icebergs during such events. Nevertheless, owing to the release of icebergs throughout the year, events of high iceberg occurrence numbers are likely reproduced This is provided that the oceanographical and meteorological conditions favoring transport of icebergs to the regions of interest are represented in the forcing fields . An example from 2003 is shown later, where extraordinarily many icebergs observed in the central Barents Sea (Zubakin et al., 2005) are found also in the model results.

The iceberg model separates between tabular and non-tabular icebergs. The IDAP database contains data on iceberg classes (Broström et al., 2009). Here, both tabular and tilted tabular icebergs are included as tabular icebergs (amounting to 59 % of the icebergs). All other iceberg classes are non-tabular.

The size of the released icebergs follows a lognormal distribution. The distribution parameters are set according to results by Zubakin et al. (2007), based on both IDAP and ICEBASE studies as well as Russian observations. Maximum lengths are set to 400 m for tabular icebergs and 200 m for non-tabular icebergs, in correspondence with observed sizes in the Barents Sea (Broström et al., 2009). Iceberg widths are generated by drawing from the distribution of length-width ratio given in Table 2. This approach preserves the characteristics of the distributions observed by Zubakin et al. (2007). As a consequence, the icebergs are not necessarily in hydrostatic equilibrium.

Following Kubat et al. (2005), we use a formulation for the geometry of non-tabular icebergs provided by Barker et al. (2004). An empirical relation between waterline length (L) and cross-sectional areas of sail and draft at different heights and depths is adopted from that study. We do not separate between subtypes (pinnacled, pyramidal, etc.)

For non-tabular icebergs, the draft is estimated as 70 % of the length. For tabular icebergs, the freeboard height is set to 0.25 of the draft. In line with Bigg et al. (1997), the draft is initially set equal to the width.

The position of the iceberg is referring to its center of gravity. The model only considers icebergs with a waterline length larger than 5 m. When icebergs melt below this limit, they are removed from the model. Furthermore, when calving from an iceberg occurs, the calved volume is removed from the model. For non-tabular icebergs, the deterioration mechanisms are defined as a reduction in water line length, which again defines the new volume and shape. For tabular icebergs, the different deterioration processes are applied on the surfaces where they act. For solar radiation, as an example, the height of the iceberg is reduced owing to surface melt. For buoyant and forced convection, the sidewalls are melting. Hence, the length and width of the icebergs are reduced accordingly. For calving of a tabular iceberg, the iceberg size is reduced corresponding to the calved volume, without change in geometric shape.

Table 2 Distribution and parameters of length and width of icebergs at their production site.

Parameter	Distribution	Mean	Standard deviation
Length	Lognormal (μ=4.04; σ=0.83)	80 m	80 m
Length/Width ratio	Normal (μ=1.578; σ=0.086)	1.578	0.086

Verifying model performance

To assess the performance and validity of the model, all drift and deterioration expressions were compared to their analytic results under constant forcing. The model parameters taken from literature were tested in the same way.

Although the length and location of the trajectories are sensitive to a range of parameters (e.g. Marchenko et al (2010) addressing the drag coefficients), no parameters were tuned against individual tracks. Instead, assumed representative coefficients were taken from literature. Unphysical trajectories were then carefully checked. For example, several trajectories running far south towards the Norwegian coast were attributed to uncertainties in the wave radiation stress formulations taken from literature. The explicit implementation of the wave radiation stress was therefore excluded. Instead, the effect is implicitly included through the choice of the wind drag coefficient (following Keghouche et al., 2010). The southward extent of the drift trajectories is also sensitive to the deterioration parameters, and careful inspection of the trajectories helped to determine representative values from the selection offered in literature. Generally, it was checked that the modeled behavior of the individual deterioration mechanisms was in agreement with observations presented in the literature, for example by comparing the relative contribution of the different deterioration processes during selected years, and the lifetime of the individual icebergs.

Number of released icebergs

During the parameter selection process, a comparison against the Abramov and Tunik (1996) atlas was done to assess the number of icebergs in the model. The Abramov and Tunik data is based on visual observations from airplanes, presented as charts showing yearly probability of occurrence (the probability that at least one iceberg is present) as well as monthly mean and maximum number of observed icebergs.

Following the initial runs of the model, the monthly maximum number of icebergs from the model was calculated in 100 by 100 km cells across the domain. The results were compared to the corresponding figures in Abramov and Tunik (1996; their Charts 3.5 and 3.9). In that study, September was the month with highest number of surveys, while May had the southernmost extent of icebergs (and thereby the highest number of icebergs in the area around Wisting). These two months were therefore used in the comparison. Model runs were then carried out over a range of percentages of the total calving rate reported for the Barents Sea. With a release rate of 3%, the model results compare fairly well to the Abramov and Tunik (1996) estimate. Particular attention was paid to the contour lines in the vicinity of Wisting. In the following, we report results from simulations using the release rate of 3% of the total calving rate reported for the Barents Sea.

Calculating iceberg occurrence

An iceberg occurrence is, by definition, an event were an iceberg drifts into a square cell centered at Wisting. According to ISO19906:2010, the cell size should be chosen to ensure that

distributions are representative for the final location of the structures to be installed at the site. Here, a square cell of 100 x 100 km size is used. The sensitivity to this choice is addressed later.

The average annual number of icebergs is determined from the iceberg drift model as follows: For each simulated year, the number of icebergs entering the cell is recorded, as well as their associated characteristics (size, velocity, position). The number of detected icebergs is divided by the number of simulated years, providing the average annual number of icebergs at Wisting. This calculation is also carried out for specific iceberg size ranges, based on their average maximum width while in the cell ($\overline{L_{max}}$).

The annual occurrence probability of icebergs is determined as the probability that at least one iceberg enters the 100 x 100 km cell during a year. This is calculated as the number of years with at least one iceberg occurring, divided by the total number of years. The annual occurrence probability is also computed for specific iceberg size ranges, based on their average maximum width while in the cell ($\overline{L_{max}}$).

RESULTS

Southward extent of icebergs

The modeled drift trajectories are demonstrated in Figure 2. Here, the iceberg drift trajectories during a year with small southward extent (2000) is compared to a year with great southward extent (2003). Generally, the southward extent of icebergs is expected to correlate with southward sea ice extent, due to the common controlling physics. Comparing the modeled drift trajectories to the sea ice maps during the model period, year by year, demonstrate that the iceberg model generally reflects this expected correlation.

Wisting is located in a region observed to be affected by icebergs during years when the conditions favour a large southward extent (Figure 2, right). Occurrence probability at Wisting is later calculated from all the trajectories of the model.

Our modelled trajectories for 2000 and 2003 in Figure 2 may be compared to corresponding results in Keghouche et al. (2010) (their Figure 8). In that study, 2000 was the year with the northernmost extent of icebergs, while 2003 had the southernmost extent. In general, our results appear to compare well with the results from Keghouche et al. (2010), particularly for the eastern Barents Sea. Icebergs observed in a region around 72°N 46° E in May 2003 (Zubakin 2005), appears to be captured by the models. Our model has a slightly more southerly extent of icebergs than Keghouche et al. (2010), during both these years. Most likely, this is due to the three times larger volume of icebergs being released in our simulations.

When doing a comparison like this between two model results, it is important to keep in mind that differences are bound to be observed. Although the model formulations are relatively similar, the initial values and the forcing data are different. The qualitative differences between model outputs observed here is therefore expected, and illustrates the usefulness of having more than one model in operation for studies like this. In total, it is convincing that two individual studies yield results that agree to the extent observed here.

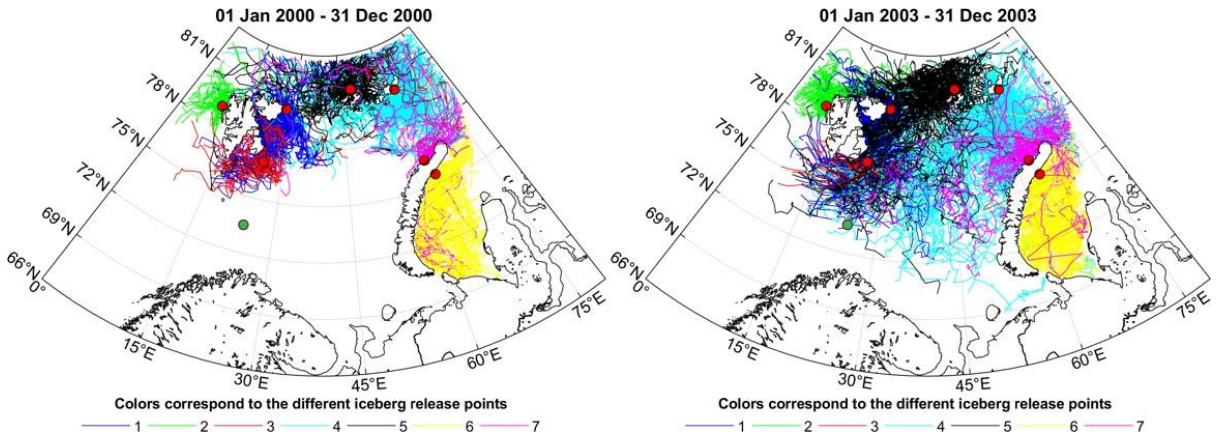

Figure 2 Model result from the years 2000 (left) and 2003 (right). The figures show modelled trajectories throughout the two years. Red points mark the iceberg release points. The green dot marks the Wisting location.

Annual probability of iceberg occurrence in the Barents Sea

The annual probability of iceberg occurrence was calculated in 100 x 100 km grid cells across the model domain. A contour plot of the annual probability of occurrence is shown in Figure 3. Comparing the map to the Abramov and Tunik (1996) observations (their Chart 3.37), shows that the model calculates higher probabilities across most of the domain. The model provides an annual probability of iceberg occurrence at Wisting around 40% (Figure 3). The Abramov and Tunik atlas shows values around 5%.

However, the general pattern of iceberg occurrence and extent produced by the model is comparable to that of the Abramov and Tunik atlas. Generally, both studies feature a relatively sharp gradient in iceberg probability across the western part of the Barents Sea. This means that estimates of iceberg probability based on different approaches for given positions are bound to differ somewhat in this region.

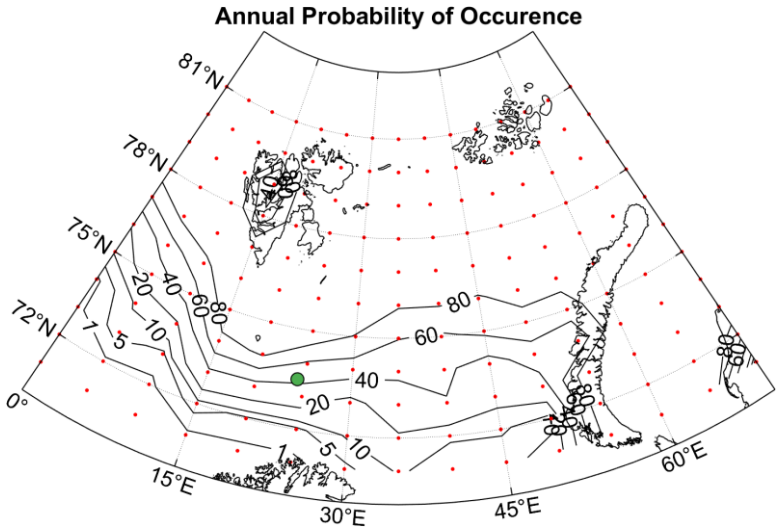

Figure 3 Annual probability (%) of iceberg occurrence from the model. The red points indicate the grid of 100 x 100 km cells were the probability of occurrence was calculated.

Iceberg occurrence at Wisting

The annual probabilities of occurrence of icebergs calculated in the 100 x 100 km grid cells were calculated for a range of size classes. The results are listed in Table 3. The annual probability of occurrence of icebergs greater than 5 m in the 100 x 100 km grid cell surrounding Wisting is found to be 0.39, or 39%. This means that on average the likelihood of at least one iceberg appearing in the 100 x 100 km cell around Wisting in any given year is 39%. This corresponds to a return period of 2.6 years. The occurrence probability decreases rapidly for larger icebergs. For icebergs greater than 20 m, the annual probability of occurrence is 0.25, or 25 %.

Table 3 Annual probability of occurrence in a 100x100 km cell surrounding Wisting, as function of iceberg size.

Annual probability of occurrence of icebergs for different iceberg sizes [m]							
> 5	> 20	> 40	> 60	> 80	> 100	> 120	> 140
0.39	0.25	0.14	0.11	0.10	0.07	0.07	0.00

The average annual number of icebergs in a 100 x 100 km cell around Wisting, as a function of the iceberg size, is presented in Table 4. The average annual number of icebergs greater than 5 m is 1.39. The number decreases rapidly with increasing iceberg sizes. For icebergs greater than 20 m, the average annual number is 0.5.

Table 4 Average annual number of icebergs in a 100x100 km cell at Wisting, as function of iceberg size.

Average annual number of icebergs for different iceberg size classes [m]							
> 5	> 20	> 40	> 60	> 80	> 100	> 120	> 140
1.39	0.50	0.25	0.21	0.14	0.07	0.07	0.00

The distributions of $\overline{L_{max}}$ and draft for icebergs in the 100 x 100 km cell around Wisting are shown in Figure 4 (left). The figure shows that a majority of the icebergs has an $\overline{L_{max}}$ in the 5 - 20 m range. The largest iceberg observed in the 100 x 100 km cell during the simulation period had an $\overline{L_{max}}$ of 140 m. Figure 4 (right) further shows the mass associated with the iceberg with different $\overline{L_{max}}$. For icebergs in the 5-20 m range, the mass range from $5 \cdot 10^{-5}$ to $2 \cdot 10^{-2}$ Mtonnes. The largest icebergs ($\overline{L_{max}}$ > 80 m) have a mass between 0.1 and 1 Mtonnes. It must be kept in mind that these numbers are based on a limited number of icebergs. The occurrence of larger icebergs cannot be ruled out.

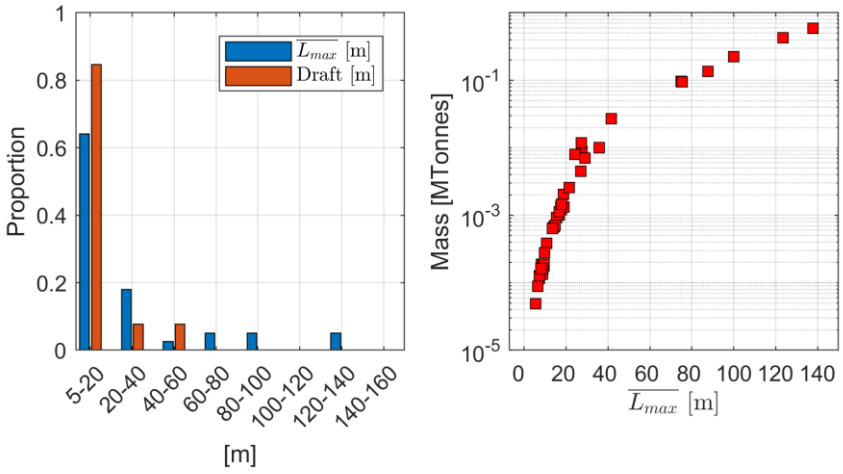

Figure 4 Proportion of icebergs in different size classes while in the 100 x 100 km cell (left), and the corresponding mass associated with each iceberg with a certain $\overline{L_{max}}$ (right).

Effect of cell size

The iceberg annual occurrence probabilities were calculated using a grid cell size of 100 x 100 km around Wisting. The effect of the cell size on the results was studied by running the calculations over a range of cell sizes (50 to 400 km). The outline of the range of cells is shown in Figure 5, with the contour lines of average annual number of icebergs in the background.

Generally, it is obvious that increasing the cell size implies increasing the number of observed icebergs. However, increasing the cell size from 50 to 100 km yields only a modest increase in occurrence probability. Increasing the cell size further beyond 100 km, shows significant sensitivity. This is explained by the fact that Wisting is located immediately south of the majority of the iceberg trajectories. As the cell size increases, the cell is expanding into parts of the Barents Sea featuring many icebergs. In conclusion, we find that the grid cell size of 100 x 100 km applied here reflects the iceberg characteristics at the Wisting position well.

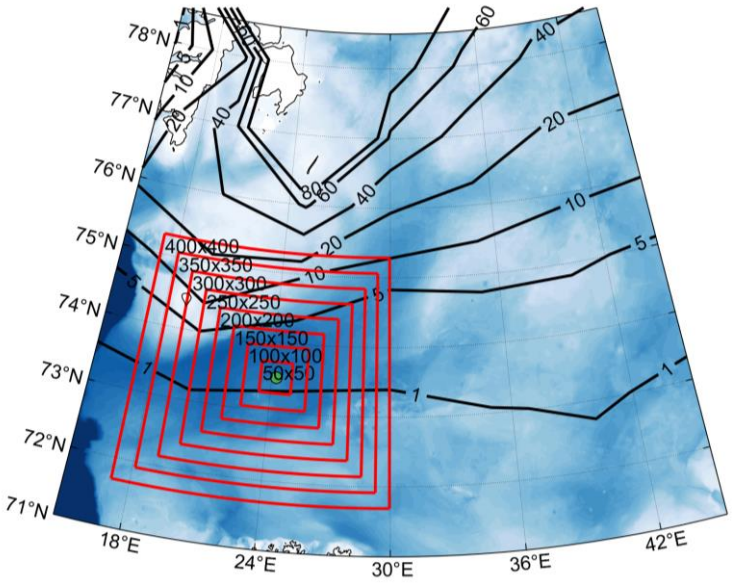

Figure 5 Outline of cells for different cell sizes. Wisting is indicated with a green point. The black lines are contour lines of the average annual number of icebergs.

DISCUSSION

Discrepancies are observed when comparing the model results to the Abramov and Tunik (1996) iceberg atlas. However, although the Abramov and Tunik atlas is based on observations, its statistics cannot immediately be taken as fully representative. It is unlikely that all icebergs were detected. It is unclear to us how this was accounted for when calculating the monthly mean numbers and annual probabilities. For example, close to Nordaustlandet, an important iceberg production site, the annual probability of occurrence is almost as low as 10% in the atlas. Since calving is expected to occur every year, this estimate appears low. Moreover, in months with few surveys (November to January) both mean and maximum monthly numbers and occurrence probabilities are very low. This is expected to be an effect of the difficulty of performing surveys during the dark season, not only a seasonal variation in the iceberg density in the Barents Sea.

The monthly maximum numbers that are reported in the Abramov and Tunik atlas are understood to be direct observations of icebergs, without averaging. As uncertainty is associated with how the annual mean and probability estimates in Abramov and Tunik (1996) were computed, the monthly maximum seems like the most meaningful number to use for a comparison to our model results. Abramov and Tunik (1996) reports that a major part of the surveys was made during the summer months, and September was the month with highest number of surveys. Their results show that May had the southernmost extent of icebergs, and thereby highest number of icebergs in the area around Wisting. These two months were therefore used for comparison when choosing the number of icebergs to release in the model.

Assuming that the surveys reported in Abramov and Tunik (1996) were unable to identify all icebergs, the annual occurrence probability at Wisting in that study should be in the lower range. In addition to possible model deficiencies, this is a likely explanation for the discrepancy between the model and atlas results.

CONCLUSIONS

Updated data on glacial ice occurrence in the Barents Sea are known to be sparse, with the Abramov and Tunik (1996) iceberg atlas being the only known source of consistent iceberg observations. Numerical iceberg drift and deterioration modeling was therefore carried out, to supplement the sparse data on iceberg occurrence near the oil and gas field Wisting (73° 30’ N 24° 14’ E).

The annual occurrence probability in a 100 x 100 km cell around Wisting was found to be 39% for icebergs greater than 5 m in size. This means that on average there is a 39% chance that at least one iceberg will appear in the 100 x 100 km cell around Wisting in a given year. This corresponds to a return period of 2.6 years. This is higher than the Abramov and Tunik (1996) iceberg atlas, which shows annual occurrence probabilities around 5%. This latter estimate is likely to be on the lower side. Hence, the new result provided by the numerical model provides an approach for objective upward adjustment of the iceberg occurrence probability at Wisting.

REFERENCES

Abramov, D.V., and Tunik, A., 1996. Atlas of Arctic icebergs: The Greenland, Barents, Kara, Laptev, East-Siberian and Chukchi Seas and the Arctic Basin. *Backbone Publishing Company.*

Barker, A., M. Sayed, and Carrieres, T., 2004. Determination of Iceberg Draft, Mass and Cross-Sectional Areas, *In proceedings of the 14th International Offshore and Polar Engineering Conference*, ISOPE 2004, Toulon, France, pp. 899-904.

Berrisford, P., D. P. Dee, P. Poli, R. Brugge, K. Fielding, M. Fuentes, P. W. Kållberg, S. Kobayashi, S. Uppala, and A. Simmons, 2011. *The ERA-Interim Archive Version 2.0. Shinfield Park*, Reading: ECMWF.

Bigg, G., Wadley, M., Stevens, D. and Johnson, A., 1997. Modelling the dynamics and thermodynamics of icebergs. *Cold Regions Science and Technology*, 26, 113-135.

Broström, G., Melsom, A., Sayed, M., and Kubat, I., 2009. Iceberg Modeling at met.no: Validation of Iceberg Model. *Report series, 17, Norwegian Meteorological Institute*, Oslo, Norway. pp. 36.

Keghouche, I., Counillon, F., and Bertino, L., 2010. Modeling dynamics and thermodynamics of icebergs in the Barents Sea from 1987 to 2005, Journal of Geophysical Research, Vol. 115, https://doi.org/10.1029/2010JC006165.

Kubat, I., Sayed, M., Savage, S. B., and Carrieres, T., 2005. An Operational Model of Iceberg Drift, *International Journal of Offshore and Polar Engineering*, Vol. 15, No. 2, pp 125-131.

Kubat, I., Sayed, M., Savage, S. B, Carrieres, T., and Crocker, G., 2007. An Operational Iceberg Deterioration Model. *In proceedings of the 17th International Offshore and Polar Engineering Conference*, ISOPE07, Lisbon, Portugal, pp. 652-657.

Røed, L. P. et al., 2015. BaSIC Technical Report 4. Part I: Evaluation of the BaSIC4 long term hindcast results. *Report series, 5, Norwegian Meteorological Institute*, Oslo, Norway.

Sharp, M. et al., 2011. Mountain glaciers and ice caps, in *"Snow, Water, Ice, and Permafrost in the Arctic (SWIPA): Climate change and the cryosphere, Arctic Monitoring and Assessment Programme (AMAP)*, Oslo, 2011.

Stern, A. A., A. Adcroft, O. Sergienko, and G. Marques (2017), Modeling tabular icebergs submerged in the ocean, *J. Adv. Model. Earth Syst.*, 9, 1948-1972, doi:10.1002/2017MS001002.

Turnbull, I. D., N. Fournier, M. Stolwijk, T. Fosnaes, and McGonigal, D., 2015. Operational Iceberg Drift Forecasting in Northwest Greenland, *Cold Regions Science and Technology*, Vol. 110, pp. 1-18.

Zubakin, G. K., A. G. Shelomentsev, D. K. Onshuus, L. I. Eide, and I. V. Buzin (2005), Spatial Distribution of Icebergs in the Barents Sea Based on Archived Data and Observations of 2003. *In proceedings of the 18th International Conference on Port and Ocean Engineering Under Arctic Conditions* (POAC) Vol. 2, Potsdam, USA, pp. 575-584

Zubakin, G. K. et al., 2007. Results of Investigations of Icebergs, Glaciers and their Frontal Zones in the Northeastern Part of the Barents Sea, *In proceedings of the19th International Conference on Port and Ocean Engineering Under Arctic Conditions (POAC07)*, Dalian, China.